Analysis of receptor oligomerization by FRAP microscopy

Sandra Dorsch, Karl-Norbert Klotz, Stefan Engelhardt, Martin J Lohse & Moritz Bünemann

Here we describe an approach to investigate di- or oligomerization of transmembrane receptors in living cells with fluorescence recovery after photobleaching (FRAP). We immobilized a defined fraction of receptors with antibodies and then measured lateral mobility of the nonimmobilized fraction by FRAP. We validated this approach with CD86 and CD28 as monomeric and dimeric reference proteins, respectively. Di- or oligomerization of G protein–coupled receptors is strongly debated. We studied human β-adrenergic receptors as prototypical G protein–coupled receptors and found that β_1-AR shows transient interactions whereas β_2-AR can form stable oligomers. We propose that this FRAP method can be widely applied to study di- or oligomerization of cell-surface proteins.

Dimerization and higher-order oligomerization has been described for various cell-surface receptors. Resonance energy transfer techniques suggest interactions between many G protein–coupled receptors (GPCRs)[1–7]. In a few cases di- or oligomerization has been convincingly linked to the function of GPCRs[2,3] or has been visualized directly using atomic force microscopy and transmission electron microscopy[4,5]. However, for many other GPCRs, di- or oligomerization is a matter of controversy[8–10].

Methodological limitations make it difficult to study several important questions, including stability of receptor complexes, fraction of interacting proteins and size of complexes[11,12]. We developed a dual-color fluorescence recovery after photobleaching (FRAP) microscopy[13]–based approach to address these questions in single living cells.

FRAP measures the diffusion of nonbleached fluorescent proteins into a small, irreversibly bleached region[14,15]. The speed and extent of FRAP depend on the lateral mobility of membrane proteins. Interaction of an immobile protein with a more mobile one will lead to a mobility reduction of the latter[16]. Here we used FRAP to analyze changes in the lateral mobility of fluorescent receptors upon immobilization of a distinct receptor fraction. Such mobility measurements have been used to study association of the cytokine receptor glycoprotein 130 and the janus kinase Jak1 (ref. 16), dissociation of G-protein subunits[17] and coupling mechanisms between receptors and Gβγ-activated ion channels[18].

Using polyclonal antibodies, we specifically immobilized receptors containing an extracellular YFP moiety in live cells. We detected a potential homomeric interaction with a second receptor bearing an intracellular CFP or Cerulean inaccessible to the antibodies. By means of dual-color FRAP we simultaneously monitored the mobility of both receptor populations. We verified the general approach using monomeric and covalent dimeric model proteins. This approach allowed us to predict the stability of interactions, to quantify the fraction of interacting proteins and to distinguish between dimerization and higher-order complexation. Using this method we found specific but unstable interactions between β_1-AR monomers. In contrast, β_2-AR formed stable higher-order oligomers.

RESULTS

Validation of the dual-color FRAP

To test the possibility of studying receptor interactions in intact cells with FRAP, we fused YFP or CFP to the extra- and intracellular part of either monomeric CD86 (ref. 19) or constitutively dimeric CD28 (refs. 20,21) proteins (**Supplementary Methods** online). When expressed in human embryonic kidney (HEK) 293T cells, FRAP microscopy showed that both receptors were mobile, independent of the fluorophore insertion site.

Incubation with a polyclonal antibody to YFP (anti-YFP) specifically immobilized extracellularly YFP-tagged CD86 (**Fig. 1a**,**b** and **Supplementary Fig. 1** online). In contrast, monoclonal antibodies to YFP restricted receptor mobility only after additional incubation with secondary antibodies directed against their Fc domain (**Fig. 1c**). Preincubation with anti-YFP did not reduce the mobility of intracellularly tagged receptors when expressed alone (**Supplementary Fig. 1**). These results verified that polyclonal antibodies to YFP are suitable to immobilize YFP-tagged receptors on the surface of living cells.

Next we examined interactions of extracellularly YFP-tagged proteins with intracellularly CFP-tagged proteins using simultaneous dual-color FRAP. We bleached YFP- and CFP-tagged receptors in a small spot and monitored the redistribution of both into the spot. We fitted the resulting FRAP curves best using a biphasic exponential equation. We measured relative expression ratios of YFP- and CFP-tagged receptors in individual cells using a reference

University of Würzburg, Institute of Pharmacology and Toxicology, Versbacher Str. 9, 97078 Würzburg, Germany. Correspondence should be addressed to M.B. (m-buenemann@toxi.uni-wuerzburg.de).

RECEIVED 4 NOVEMBER 2008; ACCEPTED 8 JANUARY 2009; PUBLISHED ONLINE 22 FEBRUARY 2009; DOI:10.1038/NMETH.1304

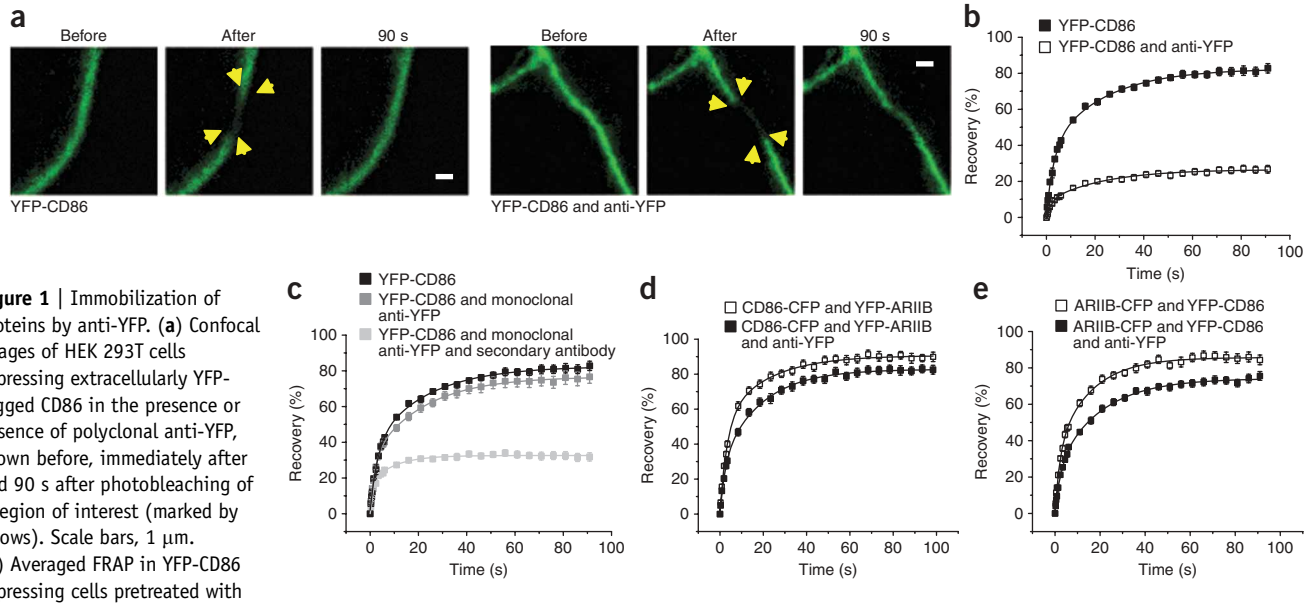

Figure 1 | Immobilization of proteins by anti-YFP. (**a**) Confocal images of HEK 293T cells expressing extracellularly YFP-tagged CD86 in the presence or absence of polyclonal anti-YFP, shown before, immediately after and 90 s after photobleaching of a region of interest (marked by arrows). Scale bars, 1 μm. (**b**) Averaged FRAP in YFP-CD86 expressing cells pretreated with ($n = 32$) or without ($n = 21$) polyclonal anti-YFP (error bars, s.e.m.). (**c**) Averaged FRAP in YFP-CD86–expressing cells pretreated with monoclonal anti-YFP ($n = 37$), with monoclonal anti-YFP and a secondary antibody ($n = 24$) or in untreated cells ($n = 21$). (**d**) Averaged FRAP in cells expressing an excess of YFP-ARIIB and CD86-CFP either with ($n = 41$) or without ($n = 28$) pretreatment with polyclonal anti-YFP. (**e**) Averaged FRAP in cells expressing YFP-CD86 and unrelated ARIIB-CFP (no antibody, $n = 23$; anti-YFP $n = 44$). All data are given as mean ± s.e.m.

construct. In each individual experiment we controlled for the efficiency of anti-YFP–induced immobilization.

To test for specificity of immobilization, we probed for effects of immobilizing the unrelated activin receptor IIb (ARIIB)[22] on the mobility of CD86-CFP (**Fig. 1d,e**). Immobilizing YFP-ARIIB only slightly restricted the mobility of CD86-CFP. Similarly, immobilizing YFP-CD86 only marginally reduced the mobility of ARIIB-CFP. We saw such minor effects with many other tested combinations of noninteracting proteins (**Supplementary Fig. 2** online) and consider them nonspecific.

As expected for monomeric proteins (**Fig. 2a**), antibody-treated cells expressing slightly more CD86-CFP than YFP-CD86 (CFP/YFP concentration = ~1.2) exhibited a robust recovery of CD86-CFP into the bleached region (80.9 ± 11.3% mobile fraction). These FRAP curves were comparable with those for CD86-CFP in cells containing antibody-immobilized YFP-ARIIB (82.8 ± 4.0%)

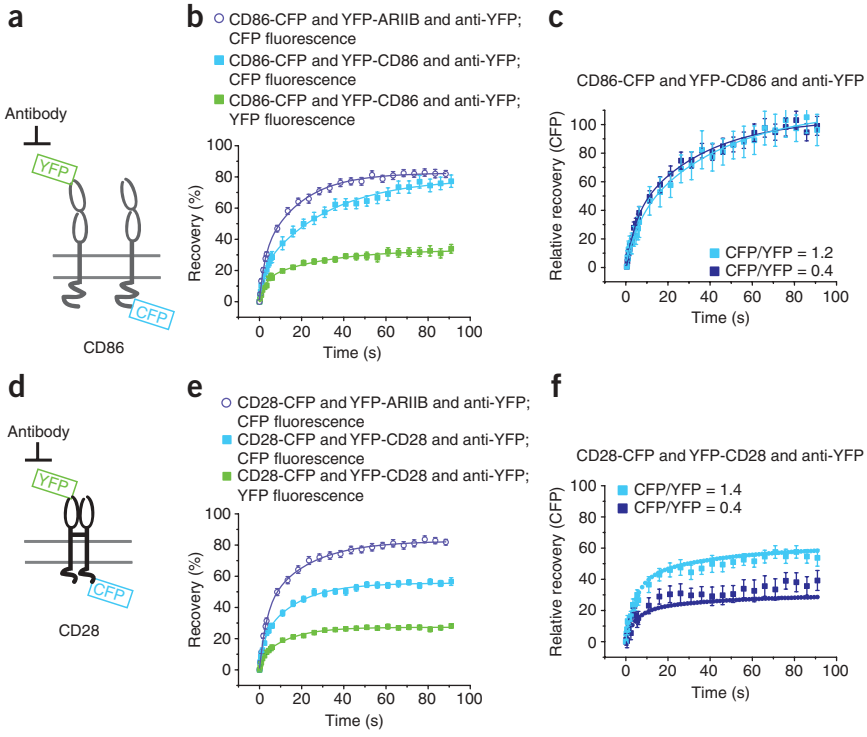

Figure 2 | Validation of the dual-color FRAP approach using monomeric and dimeric control proteins. (**a**–**f**) Schematic representations of monomeric CD86 (**a**) and dimeric CD28 (**d**). Mean FRAP curves of CD86-CFP and YFP-CD86 in cells expressing 1.2-fold more CD86-CFP over YFP-CD86 ($n = 17$) and preincubated with polyclonal anti-YFP, and of CD86-CFP expressed with antibody-immobilized YFP-ARIIB ($n = 41$) (**b**). Mean FRAP curves of CD28-CFP and YFP-CD28 in cells expressing 1.4-fold more CD28-CFP over YFP-CD28 ($n = 35$) and preincubated with polyclonal anti-YFP, and of CD28-CFP expressed with antibody-immobilized YFP-ARIIB ($n = 18$) (**e**). To account for incomplete and unspecific immobilization, data derived from **b** and **e** were corrected accordingly and normalized curves were plotted as mean relative FRAP curves for CD86-CFP (**c**) and CD28-CFP (**f**). Relative FRAP of CD86 is shown for two expression ratios of CD86-CFP and YFP-CD86 (CFP/YFP = 0.4 ± 0.02, $n = 49$; CFP/YFP = 1.2 ± 0.05, $n = 17$) (**c**). Experimental and theoretical (dotted lines) fluorescence recoveries of CD28-CFP at two expression ratios of CD28-CFP and YFP-CD28 (CFP/YFP = 0.4 ± 0.02, $n = 33$ and CFP/YFP = 1.4 ± 0.06, $n = 35$) (**f**). All data are mean ± s.e.m.

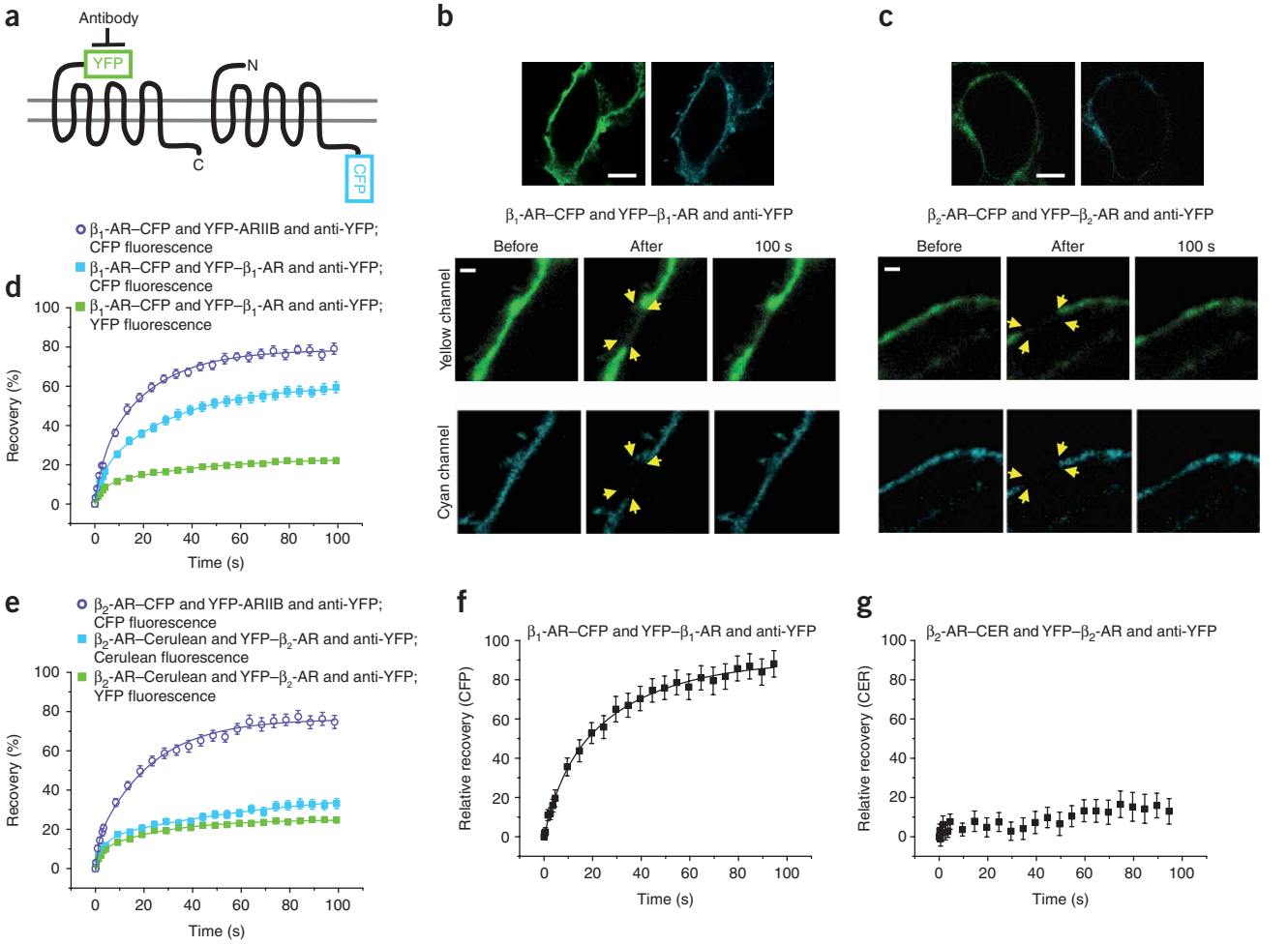

Figure 3 | Detection of di- or oligomerization of receptors by dual-color FRAP microscopy. (**a**) Schematic of YFP-receptor and receptor-CFP/Cerulean expressed in comparable amounts in cells treated with anti-YFP. (**b**,**c**) Confocal images of cells expressing β_1-AR–CFP and YFP–β_1-AR (**b**) or β_2-AR–CFP and YFP–β_2-AR (**c**) (top). The middle and lower series are images taken before, immediately after and 100 s after photobleaching of a region of interest (marked by arrows arrows); cells had been preincubated with anti-YFP. Scale bars, 5 μm (top) and 1 μm (bottom). (**d**,**e**) Mean fluorescence recovery curves of anti-YFP–preincubated cells expressing β_1-AR–CFP and YFP–β_1-AR (**d**, $n = 43$) or YFP-ARIIB (**d**, $n = 31$) or β_2-AR–Cerulean and YFP–β_2-AR (**e**, $n = 38$) or YFP-ARIIB (**e**, $n = 24$). (**f**,**g**) Curves in **d** and **e** were corrected for incomplete immobilization and for nonspecific immobilization and plotted as mean relative FRAP curves for β_1-AR–CFP (**f**) and β_2-AR–Cerulean (**g**). All data are given as mean ± s.e.m.

(**Fig. 2b**). To account for both the individual degree of immobilization efficiency in each experiment and for nonspecific immobilization effects, we calculated relative fluorescence recoveries from the FRAP curves (**Fig. 2c**) as described in Methods. The relative expression ratio of CFP- and YFP-tagged CD86 had no influence on the mobility of intracellularly tagged receptors (**Fig. 2c**). This agrees with the monomeric nature of CD86.

Likewise, the dual-color FRAP approach reported the well-known constitutive dimerization of CD28 (**Fig. 2d**). Fusion to the fluorescent proteins did not affect dimerization of CD28 (**Supplementary Fig. 3** online). Only about half (55.6 ± 3.3%) of CD28-CFP receptors (**Fig. 2e**) were mobile at 1.4-fold excess of CD28-CFP over immobilized YFP-CD28, whereas CD28-CFP expressed in cells with YFP-ARIIB was highly mobile (82.5 ± 4.6%) in antibody-treated cells. The mobility restriction of intracellularly tagged CD28 receptors depended on the ratio of CFP- over YFP-tagged receptors. At CFP/YFP of ~1.4, 61.2 ± 5.6% of CD28-CFP were mobile, whereas at CFP/YFP of ~0.4, the mobility of CD28-CFP was reduced to 39.6 ± 3.7% (**Fig. 2f**), indicating a specific interaction between CD28 monomers. Based on theoretical calculations for a constitutive dimer (**Supplementary Methods**) we predicted mobile fractions of 28.6% and 58.3% for CD28-CFP for CFP/YFP of 0.4 and 1.4, respectively (**Fig. 2f**). These curves were in good agreement with the experimental data.

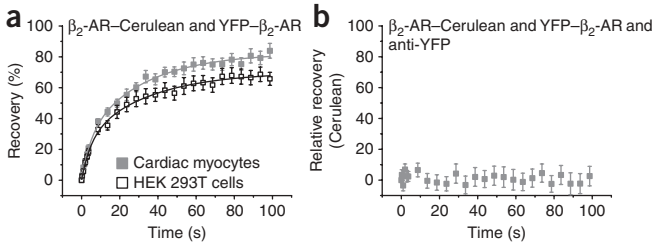

Figure 4 | β_2-AR homomeric interaction in cardiac myocytes. (**a**) Mean FRAP of β_2-AR–Cerulean in untreated cardiac myocytes ($n = 24$) and in untreated HEK 293T cells ($n = 15$) expressing β_2-AR–Cerulean and YFP-β_2-AR. (**b**) Mean FRAP of β_2-AR–Cerulean in cardiac myocytes expressing β_2-AR–Cerulean and YFP–β_2-AR after pretreatment with anti-YFP ($n = 31$). Data are mean ± s.e.m.

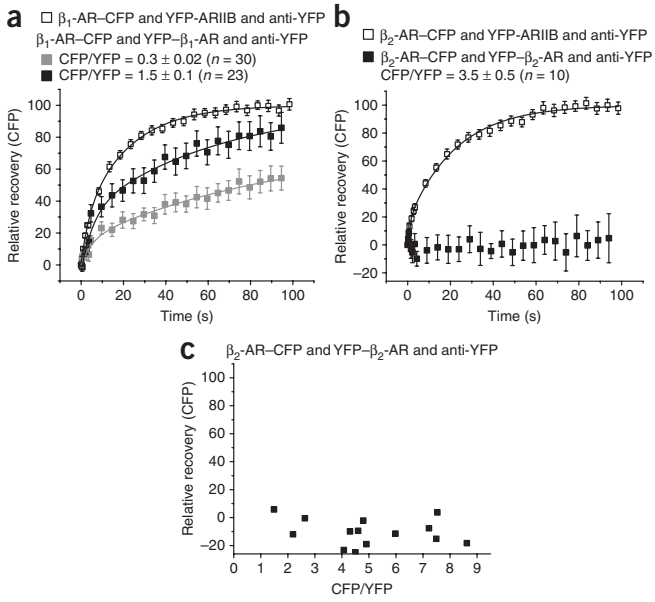

Figure 5 | Effects of expression ratios on FRAP of β_1-AR and β_2-AR. (**a**) FRAP curves are shown for two expression ratios of β_1-AR–CFP over YFP–β_1-AR. The normalized FRAP curve of β_1-AR–CFP ($n = 31$) in antibody-treated cells expressing YFP-ARIIB is also shown. (**b**) FRAP curve for almost fourfold excess of β_2-AR–CFP over YFP–β_2-AR. The normalized FRAP curve of β_2-AR–CFP ($n = 24$) in antibody-treated cells expressing YFP-ARIIB is also shown. Data are given as mean ± s.e.m. (**c**) Relative recovery 84 s after photobleaching of β_2-AR–CFP at all measured expression ratios ($n = 14$).

In summary, the experimental FRAP data on CD86 and CD28 agreed well with predicted values, verifying this dual-color FRAP approach as a reliable method to study membrane protein dimerization.

β_1-AR and β_2-AR homomeric interactions

Next we applied the approach to β-AR (**Fig. 3a**). We fused CFP and YFP either to the intracellular C terminus or the extracellular N terminus of β_1-AR and β_2-AR (**Supplementary Methods**). These constructs were functional and exhibited wild type–like expression and signaling properties (**Supplementary Fig. 4** online). We verified that treatment with polyclonal anti-YFP selectively restricted the mobility of extracellularly tagged β-AR (**Supplementary Fig. 5** online).

Cells expressing equivalent amounts of β_1-AR–CFP and YFP–β_1-AR exhibited marked FRAP of β_1-AR–CFP into the bleached region, whereas only a minor fraction of YFP–β_1-AR was mobile after incubation with antibody (**Fig. 3b**). In contrast, anti-YFP–treated cells expressing equivalent amounts of β_2-AR–Cerulean and YFP-β_2-AR showed only a marginal FRAP of both YFP–β_2-AR and β_2-AR–Cerulean (**Fig. 3c**; also compare **Fig. 3d**,**e**). Calculation of relative fluorescence recoveries revealed that immobilization of YFP–β_1-AR restricted the mobility of β_1-AR–CFP receptors by about 15% (**Fig. 3f**) whereas immobilization of YFP-β_2-AR receptors nearly completely immobilized β_2-AR–Cerulean receptors (**Fig. 3g**); we detected no recovery of β_2-AR–Cerulean mobility even after 5 min (data not shown).

We excluded artificial aggregation of β_2-AR owing to altered fluidity of membrane lipids at room temperature (18–22 °C) by conducting the FRAP experiments at 37 °C (**Supplementary Fig. 6** online). Furthermore, the type of GFP variant used as intracellular or extracellular tag had no influence on the results (**Supplementary Fig. 6**). The di- or oligomerization state of β-AR was independent of receptor activation as neither 10 μM isoproterenol (agonist) nor 1 μM propranolol (antagonist) notably affected the observed interaction patterns of both β_1- and β_2-AR (data not shown).

We also examined whether β_2-AR interaction also occurs in neonatal rat cardiac myocytes, which endogenously express the receptor. The mobility of β_2-AR–Cerulean was slightly higher in cardiac myocytes compared to that in HEK 293T cells (**Fig. 4a**). Nevertheless, antibody-induced immobilization of YFP-β_2-AR in cardiac myocytes efficiently coimmobilized β_2-AR–Cerulean (**Fig. 4b**), suggesting that oligomerization of β_2-AR may also occur in native tissue.

Stability of receptor complexes

So far we showed that a majority of β_1-AR–CFP receptors remained mobile after immobilization of expressed YFP–β_1-AR receptors (**Fig. 3f**), suggesting at most a weak or transient interaction between these receptors. To further characterize this interaction we determined relative expression ratios and classified FRAP curves according to the expression ratios, as we did for CD86 and CD28.

β_1-AR interaction depended on the expression ratios of extracellularly and intracellularly tagged receptors (**Fig. 5a**). The immobilization of YFP–β_1-AR receptors had little effect on the extent of immobilization of β_1-AR-CFP, but the fluorescence recovery time was substantially increased with decreasing CFP/YFP. At CFP/YFP of ~0.3 in antibody-treated cells, conditions making β_1-AR-CFP/β_1-AR–CFP homodimer formation unlikely, the time constant for β_1-AR–CFP increased to 155 s compared to 22 s in cells co-expressing YFP-ARIIB and preincubuated with antibody. These results demonstrated that β_1-AR di- or oligomerization is unstable and dynamic on a timescale of seconds.

Dimerization versus oligomerization of β-AR

Next we examined the fluorescent protein–tagged receptors at different relative expression ratios. Even in cells expressing a 3.5-fold excess of β_2-AR-CFP over antibody-immobilized YFP-β_2, we detected no diffusion of β_2-AR-CFP into the bleached area (**Fig. 5b**). For exclusive and stable dimer formation, 78% of β_2-AR-CFP should remain mobile under these conditions. Furthermore, at all measured CFP/YFP, the mobility of β_2-AR-CFP was completely restricted (**Fig. 5c**). This suggests that one YFP-β_2-AR receptor was probably able to restrict the mobility of at least four β_2-AR-CFP receptors indicating higher-order complexes of β_2-AR.

DISCUSSION

We specifically immobilized receptor-YFP fusion proteins by binding polyclonal antibodies to different epitopes on YFP molecules. In contrast, binding of monoclonal antibodies to YFP-expressing proteins was not sufficient for immobilization. FRAP curves for monomeric and dimeric fluorescent receptors were in good agreement with the theoretically predicted recoveries, validating antibody-induced immobilization. The slight discrepancy between

experimental and theoretical recovery of CD28 for CFP/YFP of ~0.4 might reflect incomplete dimerization.

The extent and functional relevance of interactions between GPCRs is still a matter of controversy[8–10]. Dimerization or oligomerization of GPCRs is not generally necessary for receptor-mediated G-protein activation[23,24]. However, an increasing number of examples suggest receptor interactions in living cells, which in some instances are required for proper function[2,3].

For β_1-AR–CFP we observed a specific but transient interaction. Moreover, a major fraction of β_1-AR–CFP receptors exhibited delayed FRAP, suggesting that most receptors engage in these transient interactions. The slowing of FRAP owing to immobilization of a fraction of receptors was an indirect measure of the stability of the oligomeric receptor complex. The speed of FRAP of intracellularly tagged receptors strongly correlated with the expression ratio of intra- over extracellularly fluorescent protein–tagged receptors. This contrasted with the results obtained for both monomeric CD86 and covalent dimeric CD28, suggesting non-stable interactions between β_1-AR.

For β_2-AR we found extensive and stable interactions of the entire receptor population both in HEK 293T cells and cardiac myocytes. Neither the stability nor the extent of oligomerization was affected by agonists or antagonists. These results are supported by resonance energy transfer studies suggesting stable oligomerization of β_2-AR[6,7] and the observation that these receptors internalize as oligomeric entities[25]. Our results indicated the existence of stable higher-order complexes containing probably more than 4–5 receptors. This notion is supported by the surprising lack of FRAP of intracellularly tagged β_2-AR even when expressed in excess of immobilized extracellularly tagged receptors.

The exact size and composition of the receptor complexes remain to be examined. The titration of fluorescent β_2-AR was restricted owing to saturation of β_2-AR–Cerulean expression and unfavorable signal-to-noise ratios at low expression of YFP–β_2-AR. Furthermore, insufficient immobilization at very low epitope densities limited the dynamic range of the assay. The apparent higher-order complexation of β_2-AR detected by FRAP might reflect indirect clustering of several receptors into larger complexes or oligomerization of receptors or of receptor dimers. The FRAP approach does not allow one to differentiate between these possibilities.

We obtained marked differences between β_1-AR and β_2-AR under very similar experimental conditions, including identical immobilization procedures. Absolute expression levels of β_2-AR were even slightly lower than for β_1-AR (**Supplementary Fig. 4**) arguing against crowding phenomena being responsible for their stable oligomerization. However, similar to resonance energy transfer and many other approaches, our method is based on exogenous expression of tagged proteins. Therefore, expression of these proteins may potentially exceed endogenous receptor expression by several fold, which implies that some caution needs to be applied in interpretation of results.

Immobilization of membrane proteins always led to a small degree of immobilization of unrelated proteins (**Supplementary Fig. 2**). This might reflect an increase in stability, size or number of membrane barriers, or reflect interactions with cytoskeletal proteins[15,26]. Immobilization of β_2-AR led to a slightly larger effect on the mobility of unrelated membrane proteins, which might be attributed to the formation of larger complexes of β_2-AR.

The modified dual-color FRAP approach we presented here is complementary to resonance energy transfer techniques. The FRAP approach allowed us to make predictions about the stability of interactions, to quantify the fraction of interacting proteins and thereby to distinguish between dimerization and higher order complexation of receptors.

METHODS

Antibody treatment. Cells grown on coverslips were washed three times with BE buffer[17] (150 mM NaCl, 2.5 mM KCl, 10 mM HEPES, 12 mM glucose, 0.5 mM $CaCl_2$ and 0.5 mM $MgCl_2$) or modified BE buffer (containing 100 mM KCl and 52.5 mM NaCl, respectively). Then we incubated cells at 22 °C or 37 °C for 0.5 h with antibodies diluted 1:100 in BE buffer supplemented with 2.5% bovine serum albumin. We used polyclonal (biotinylated goat anti-GFP) or monoclonal (mouse anti-GFP) antibodies (Rockland). For cross-linking monoclonal antibodies we used a goat anti-mouse immunoglobulin gamma (Dianova) in a subsequent incubation (**Fig. 1c**).

FRAP microscopy. We mounted coverslips in BE buffer onto a Leica TCS SP5 scanning confocal microscope with a ×63, 1.4 numerical aperture (NA) oil-immersion objective and performed experiments at 22 °C unless otherwise indicated. For excitation of CFP and Cerulean, we used a 405 nm diode laser; for excitation of YFP we used the 514 nm argon ion laser. We detected emission at 461–488 nm and 518–600 nm, respectively. The settings for scanning were scanning at 1,000 Hz, ×10 zoom, image format 256 × 256 pixels, pinhole 95.55 µm. We adjusted laser intensity for photobleaching to obtain 50% to 75% loss of fluorescence in the 3 µm × 1 µm rectangular bleached region in the equatorial plane of the cell membrane. To allow for rapid bleaching, we used high laser intensities for a single bleaching scan (0.278 s). We collected images before and after bleaching using low laser intensities and monitored FRAP for 80 s to 5 min. We corrected data from dual-color FRAP experiments for bleedthrough of CFP or Cerulean into the YFP channel.

Determination of expression ratios of fluorophores. We collected CFP and YFP images at fixed excitation and emission parameters, and analyzed the ratio of CFP/YFP emission in a region selected to be bleached subsequently. This ratio was compared to that of control cells expressing fusion proteins containing extracellular YFP and intracellular CFP in a single protein.

Analysis of dual-color FRAP measurements. To analyze dual-color FRAP experiments we obtained the FRAP curve of each fluorophore as described in **Supplementary Methods**. To assess the fraction of interacting receptors we considered two imperfect experimental situations: first, cross-linking of extracellularly tagged proteins led to a minor decrease in mobility of noninteracting proteins (nonspecific immobilization; **Fig. 1d**,**e** and **Supplementary Fig. 2**). We corrected data from each individual experiment for the respective fraction (**Supplementary Fig. 7** online). Second, the mobility of extracellularly tagged receptors was not completely restricted by antibody treatment. We therefore subtracted FRAP curves for directly antibody-immobilized receptors from those of intracellular tagged receptors corrected for nonspecific immobilization. We

set the maximum of the resulting curve to 100% relative recovery (**Supplementary Fig. 7**).

Curve fitting. We averaged the resulting FRAP curves, plotted them as mean ± s.e.m. and fitted them best using a bi-exponential equation (Origin 6.1; OriginLab). The biphasic shape of FRAP curves is not completely understood, but has been described elswhere[27,28]. The indicated errors of mobile fractions and time constants are standard errors of the parameters of the fit. The fraction under the asymptote of the FRAP curve represents the mobile fraction, and the portion above represents the immobile fraction. We excluded experiments in which the extracellularly tagged receptors were not sufficiently restricted after antibody treatment (>40% FRAP).

Additional methods. Descriptions of vector constructs, cell culture and transfection, radioligand binding, measurement of adenylyl cyclase activity, western blotting, analysis of FRAP measurements and theoretical FRAP are available in **Supplementary Methods**.

Note: Supplementary information is available on the Nature Methods website.

ACKNOWLEDGMENTS

We thank N.A. Lambert (Medical College of Georgia) for methodical advice and him as well as U. Zabel (University of Wuerzburg), C. Krasel (University of Reading) and S.J. Davis (Oxford University) for providing cDNA constructs. This work was funded by the Deutsche Forschungsgemeinschaft (SFB 487 TPA1 to M.J.L. and TPA10 to M.B.).

AUTHOR CONTRIBUTIONS

S.D. performed and analyzed experiments; S.D. and M.B. designed experiments; K.-N.K. and M.J.L. contributed important ideas to the experiments; S.E. provided neonatal rat cardiac myocytes and some materials; S.D., M.B., K.-N.K. and M.J.L. wrote the manuscript.

Published online at http://www.nature.com/naturemethods/
Reprints and permissions information is available online at http://npg.nature.com/reprintsandpermissions/

1. Angers, S., Salahpour, A. & Bouvier, M. Dimerization: an emerging concept for G protein-coupled receptor ontogeny and function. *Annu. Rev. Pharmacol. Toxicol.* **42**, 409–435 (2002).
2. Jones, K.A. *et al.* $GABA_B$ receptors function as a heteromeric assembly of the subunits $GABA_BR1$ and $GABA_BR2$. *Nature* **396**, 674–679 (1998).
3. White, J.H. *et al.* Heterodimerization is required for the formation of a functional $GABA_B$ receptor. *Nature* **396**, 679–682 (1998).
4. Fotiadis, D. *et al.* Atomic-force microscopy: rhodopsin dimers in native disc membranes. *Nature* **421**, 127–128 (2003).
5. Suda, K., Filipek, S., Palczewski, K., Engel, A. & Fotiadis, D. The supramolecular structure of the GPCR rhodopsin in solution and native disc membranes. *Mol. Membr. Biol.* **21**, 435–446 (2004).
6. Angers, S. *et al.* Detection of beta 2-adrenergic receptor dimerization in living cells using bioluminescence resonance energy transfer (BRET). *Proc. Natl. Acad. Sci. USA* **97**, 3684–3689 (2000).
7. Mercier, J.F., Salahpour, A., Angers, S., Breit, A. & Bouvier, M. Quantitative assessment of beta 1- and beta 2-adrenergic receptor homo- and heterodimerization by bioluminescence resonance energy transfer. *J. Biol. Chem.* **277**, 44925–44931 (2002).
8. James, J.R., Oliveira, M.I., Carmo, A.M., Iaboni, A. & Davis, S.J. A rigorous experimental framework for detecting protein oligomerization using bioluminescence resonance energy transfer. *Nat. Methods* **3**, 1001–1006 (2006).
9. Bouvier, M., Heveker, N., Jockers, R., Marullo, S. & Milligan, G. BRET analysis of GPCR oligomerization: newer does not mean better. *Nat. Methods* **4**, 3–4 author reply 4 (2007).
10. Salahpour, A. & Masri, B. Experimental challenge to a 'rigorous' BRET analysis of GPCR oligomerization. *Nat. Methods* **4**, 599–600 author reply 601 (2007).
11. Lopez-Gimenez, J.F., Canals, M., Pediani, J.D. & Milligan, G. The alpha1b-adrenoceptor exists as a higher-order oligomer: effective oligomerization is required for receptor maturation, surface delivery, and function. *Mol. Pharmacol.* **71**, 1015–1029 (2007).
12. Maurel, D. *et al.* Cell-surface protein-protein interaction analysis with time-resolved FRET and snap-tag technologies: application to GPCR oligomerization. *Nat. Methods* **5**, 561–567 (2008).
13. Picard, D., Suslova, E. & Briand, P.A. 2-color photobleaching experiments reveal distinct intracellular dynamics of two components of the Hsp90 complex. *Exp. Cell Res.* **312**, 3949–3958 (2006).
14. Lippincott-Schwartz, J., Snapp, E. & Kenworthy, A. Studying protein dynamics in living cells. *Nat. Rev. Mol. Cell Biol.* **2**, 444–456 (2001).
15. Reits, E.A. & Neefjes, J.J. From fixed to FRAP: measuring protein mobility and activity in living cells. *Nat. Cell Biol.* **3**, E145–E147 (2001).
16. Giese, B. *et al.* Long term association of the cytokine receptor gp130 and the Janus kinase Jak1 revealed by FRAP analysis. *J. Biol. Chem.* **278**, 39205–39213 (2003).
17. Digby, G.J., Lober, R.M., Sethi, P.R. & Lambert, N.A. Some G protein heterotrimers physically dissociate in living cells. *Proc. Natl. Acad. Sci. USA* **103**, 17789–17794 (2006).
18. Lober, R.M., Pereira, M.A. & Lambert, N.A. Rapid activation of inwardly rectifying potassium channels by immobile G-protein-coupled receptors. *J. Neurosci.* **26**, 12602–12608 (2006).
19. Bhatia, S., Edidin, M., Almo, S.C. & Nathenson, S.G. Different cell surface oligomeric states of B7–1 and B7–2: implications for signaling. *Proc. Natl. Acad. Sci. USA* **102**, 15569–15574 (2005).
20. Aruffo, A. & Seed, B. Molecular cloning of a CD28 cDNA by a high-efficiency COS cell expression system. *Proc. Natl. Acad. Sci. USA* **84**, 8573–8577 (1987).
21. Lazar-Molnar, E., Almo, S.C. & Nathenson, S.G. The interchain disulfide linkage is not a prerequisite but enhances CD28 costimulatory function. *Cell. Immunol.* **244**, 125–129 (2006).
22. Zimmerman, C.M. & Mathews, L.S. Activin receptors: cellular signalling by receptor serine kinases. *Biochem. Soc. Symp.* **62**, 25–38 (1996).
23. Whorton, M.R. *et al.* A monomeric G protein-coupled receptor isolated in a high-density lipoprotein particle efficiently activates its G protein. *Proc. Natl. Acad. Sci. USA* **104**, 7682–7687 (2007).
24. Ernst, O.P., Gramse, V., Kolbe, M., Hofmann, K.P. & Heck, M. Monomeric G protein–coupled receptor rhodopsin in solution activates its G protein transducin at the diffusion limit. *Proc. Natl. Acad. Sci. USA* **104**, 10859–10864 (2007).
25. Sartania, N., Appelbe, S., Pediani, J.D. & Milligan, G. Agonist occupancy of a single monomeric element is sufficient to cause internalization of the dimeric β_2-adrenoceptor. *Cell. Signal.* **19**, 1928–1938 (2007).
26. Webb, W.W., Barak, L.S., Tank, D.W. & Wu, E.S. Molecular mobility on the cell surface. *Biochem. Soc. Symp.* **46**, 191–205 (1981).
27. Sprague, B.L. & McNally, J.G. FRAP analysis of binding: proper and fitting. *Trends Cell Biol.* **15**, 84–91 (2005).
28. Saxton, M.J. Anomalous subdiffusion in fluorescence photobleaching recovery: a Monte Carlo study. *Biophys. J.* **81**, 2226–2240 (2001).